

Internet Traffic Volumes Are Not Gaussian - They Are Log-Normal: An 18-Year Longitudinal Study With Implications for Modelling and Prediction

Mohammed Alasmar
Department of Informatics
University of Sussex
Brighton, UK
m.alasmar@sussex.ac.uk

Richard Clegg
School of Computer Science
Queen Mary University of London
London, UK
r.clegg@qmul.ac.uk

Nickolay Zakhleniuk
School of Computer Science
University of Essex
Colchester, UK
naz@essex.ac.uk

George Parisis
Department of Informatics
University of Sussex
Brighton, UK
g.paris@sussex.ac.uk

Abstract—Getting good statistical models of traffic on network links is a well-known, often-studied problem. A lot of attention has been given to correlation patterns and flow duration. The distribution of the amount of traffic per unit time is an equally important but less studied problem. We study a large number of traffic traces from many different networks including academic, commercial and residential networks using state-of-the-art statistical techniques. We show that traffic obeys the log-normal distribution which is a better fit than the Gaussian distribution commonly claimed in the literature. We also investigate an alternative heavy-tailed distribution (the Weibull) and show that its performance is better than Gaussian but worse than log-normal. We examine anomalous traces which exhibit a poor fit for all distributions tried and show that this is often due to traffic outages or links that hit maximum capacity. We demonstrate that the data we look at is stationary if we consider samples of 15 minutes or even one hour long. This gives confidence that we can use the distributions for estimation and modelling purposes.

We demonstrate the utility of our findings in two contexts: predicting that the proportion of time traffic will exceed a given level (for service level agreement or link capacity estimation) and predicting 95th percentile pricing. We also show that the log-normal distribution is a better predictor than Gaussian or Weibull distributions in both contexts.

Index Terms—Traffic modelling, network planning, bandwidth provisioning, traffic billing

I. INTRODUCTION

Internet traffic characterisation is an important problem for network researchers and vendors. The subject has a long history. Early works [1], [2] discovered that the correlation structure of traffic exhibits self-similarity and that the durations of individual flows of packets show heavy-tails [3]. These works were later challenged and refined (see Section VII for a summary). By comparison, the distribution of the amount of traffic present on a link in a given time period has seen comparatively less research interest. This is surprising as correct traffic statistics can be extremely useful in network planning. In this paper we use a rigorous statistical approach to fitting a statistical distribution to the amount of traffic within a given time period. Formally, we choose some timescale T and let X_i be the amount of traffic seen in the time period $[iT, (i + 1)T)$. We investigate the distribution of the random

variable X over a wide range of values of T . We show that the distribution of the variable has considerable implications for network planning; for assessing how often a link is over capacity and in particular for service level agreements (SLAs), and for traffic pricing, particularly using the 95th percentile scheme [4].

Previous authors have claimed that X has a normal (or Gaussian) distribution [5]–[7]. Others claim X is Gaussian plus a tail associated with bursts [8], [9]. All these studies are based on straightforward goodness-of-fit tests (e.g., Quantile-Quantile (Q-Q) plots) and relevant correlation tests that are used to assess how well captured traffic traces are fitted to Gaussian or heavy-tailed distributions. As discussed in [10], these statistical approaches can produce a substantially inaccurate assessment about whether samples follow a Gaussian/heavy-tailed or not. This is because the difference in these distributions lies in the behaviour of the tail where there can be relatively few samples, therefore large amounts of data and careful statistical handling are both important to determine the correct distribution [10].

In this paper, we use a well-established statistical methodology [10] to show that a log-normal¹ distribution is a better fit than Gaussian or Weibull² for the vast majority of traces. This holds over a wide range of timescales T (from 5 msec to 5 sec) [11]. In contrast to existing literature (e.g. [5], [6], [8]), we extensively test all studied time series for stationarity using state of the art techniques and examine their trend and seasonality components. The majority of the 15 minutes and 1 hour long traces in the dataset are stationary at all aggregation timescales. This paper is the most comprehensive investigation of this phenomenon the authors know about. We study a large number of publicly available traces from a diverse set of locations (including commercial, academic and residential

¹A variable X has a log-normal distribution if its logarithm is normally distributed $\ln(X) \sim N(\mu, \sigma^2)$ where $\mu \in \mathbb{R}$ is the mean and $\sigma > 0$ is the standard deviation of the distribution.

²A variable X has a Weibull distribution with parameters $k > 0$ (known as shape) and $\lambda > 0$ (known as scale) if its probability density function follows $f(x) = \frac{k}{\lambda} \left(\frac{x}{\lambda}\right)^{k-1} \exp(-(x/\lambda)^k)$ when $x \geq 0$ and is 0 otherwise.

networks) with different link speeds and spanning the last 18 years. There are a small number of anomalous traces in our datasets where the distribution deviates from log-normal and we find that this occurs when a link spends considerable time either having an outage or completely at maximum capacity. These anomalous traces can be presented using a bimodal distribution.

We show how often a link following a given distribution will be over a given capacity and show that our approach improves greatly on results assuming traffic follows a Gaussian distribution. We further show that if an ISP wishes to estimate future transit bills that use the 95th percentile billing scheme, then the log-normal is a better model than the Gaussian distribution.

The structure of the paper is as follows. In Section II we describe the datasets used. In Section III we describe our best-practice procedure for fitting traffic and demonstrate that log-normal is the best fit distribution for our traces under a variety of circumstances. We examine those few traces that do not follow this distribution and find it occurs when a link spends considerable time either having an outage or completely at maximum capacity. In Section IV we test all studied time series for stationarity at different time scales. In Section V we demonstrate that the log-normal distribution is the most useful for estimating how often a link is over capacity. In Section VI we show that the log-normal distribution provides good estimates when looking at 95th percentile pricing. In Section VII we give related work. Finally, Section VIII gives our conclusions.

II. NETWORK TRAFFIC TRACES

A key contribution of our work stems from the spatial and temporal diversity of the studied traces. The studied dataset spans a period of 18 years and comprises 232 traces.

CAIDA traces. We have used 27 CAIDA traces captured at an Internet data collection monitor which is located at an Equinix data centre in Chicago [12]. The data centre is connected to a backbone link of a Tier 1 ISP. The monitor records an hour-long traces four times a year, usually from 13:00 to 14:00 UTC. Each trace contains billions of IPv4 packets, the headers of which are anonymised. The average captured data rate is 2.5 Gbps. At the time of capturing, the monitored link had a capacity of 10 Gbps. Traces were captured between 2013 and 2016.

MAWI traces. The MAWI archive [13] consists of a collection of Internet traffic traces, captured within the WIDE backbone network that connects Japanese universities and research institutions to the Internet. Each trace consists of IP level traffic observed daily from 14:00 to 14:15 at a vantage point within WIDE. Traces include anonymised IP and MAC headers, along with an *ntpd* timestamp [13]. We have looked at 110 traces (each one being 15 minutes long). Traces were captured between 2014 and 2020. On average, each trace consists of 70 million packets; the average captured data rate is 422 Mbps. The monitored link had a capacity of 1 Gbps.

For the stationarity tests presented in Section IV we used a 24-hour long Mawi trace³. This trace was captured on 09/05/2018 at samplepoint-G which monitors a 10 Gbps link to DIX-IE⁴.

Twente University traces. We used 40 traffic traces captured at five different locations (8 traces from each location). Traces are diverse in terms of the link rates, types of users and capture time [14]. Each trace is 15 minutes long. The first location is a residential network with a 300 Mbps link, which connects 2000 students (each one having a 100 Mbps access link); traces were captured in July 2002. The second location is a research institute network with a 1 Gbps link which connects 200 researchers (each one having a 100 Mbps access link); traces were captured between May and August 2003. The third location is at a large college with a 1 Gbps link which connects 1000 employees (each one having a 100 Mbps access link); traces were captured between February and July 2004. The fourth location is an ADSL access network with a 1 Gbps ADSL link used by hundreds of users (each one having a 256 Kbps to 8 Mbps access link); traces were captured between February and July 2004. The fifth location is an educational organisation with a 100 Mbps link connecting 135 students and employees (each one having a 100 Mbps access link); traces were captured between May and June 2007.

Waikato University VIII traces. The Waikato dataset consists of traffic traces captured by the WAND group at the University of Waikato, New Zealand [15]. The capture point is at the link interconnecting the University with the Internet. All of the traces were captured using software that was specifically developed for the Waikato capture point and a DAG 3 series hardware capture card. All IP addresses within the traces are anonymised. In our study, we have used 30 traces captured between April 2011 and November 2011.

Auckland University IX traces. The Auckland dataset consists of traffic traces captured by the WAND group at the University of Waikato [16]. The traces were collected at the University of Auckland, New Zealand. The capture point is at the link interconnecting the University with the Internet. All IP addresses within the traces are anonymised. In our study, we have used 25 traces captured in 2009.

III. FITTING A STATISTICAL DISTRIBUTION TO INTERNET TRAFFIC DATA

In this section we present an extensive statistical analysis applied to the datasets described in the previous section. The aim is to discover which statistical distribution best fits the traces. In contrast to the existing research (see Section VII), we are basing our analysis on the framework proposed by Clauset et al. [10], a comprehensive statistical framework developed specifically for testing power-law behaviour in empirical data⁵. The framework combines maximum-likelihood fitting methods with goodness-of-fit tests based on the Kolmogorov–Smirnov statistic and likelihood ratios. The method reliably

³<https://mawi.wide.ad.jp/mawi/dit/dit2018-G/>

⁴<http://two.wide.ad.jp/>

⁵We have used the source code discussed in [17].

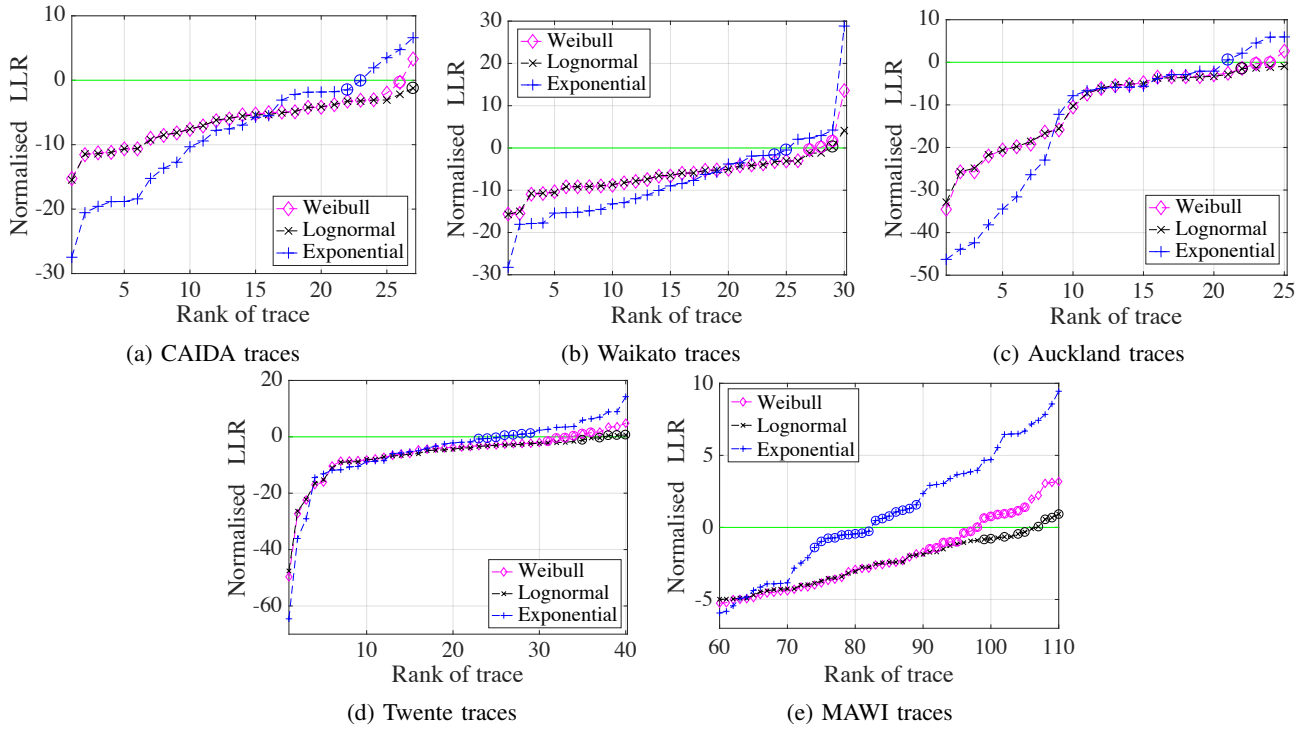


Fig. 1: Normalised Log-Likelihood Ratio (LLR) test results for all studied traces and candidate distributions. Aggregation timescale T is 100 msec. Circled points in the plot are the ones with p -value greater than 0.1; i.e. likelihood test is inconclusive with respect to fitting any of the candidate distributions to the traffic data.

tests whether the power-law distribution is the best model for a specific dataset, or, if not, whether an alternative statistical distribution (e.g., log-normal, exponential, Weibull) is. The framework performs the tests described above as follows: (1) the parameters of the power-law model are estimated for a given dataset; (2) the goodness-of-fit between the data and the power-law is calculated, under the hypothesis that the power-law is the best fit to the provided traffic samples. If the resulting p -value is greater than 0.1 the hypothesis is accepted (i.e. the power law is a plausible fit to the given data), otherwise the hypothesis is rejected; (3) alternative distributions are tested against the power-law as a fit to the data by employing a likelihood ratio test.

For the vast majority of the traces examined, the hypothesis was rejected; i.e. the power-law distribution was not a good fit. Consequently, we investigate alternative distributions by performing the likelihood ratio (LLR) test (following Clauset’s methodology), as follows:

$$\mathfrak{R}, p = \text{fit.distributionCompare}(\text{powerlaw}, \text{alternative})$$

where \mathfrak{R} is the normalised LLR⁶ between the power-law and alternative distributions and p is the significance value for this test. \mathfrak{R} is positive if the power-law distribution is a better fit for the data, and negative if the alternative distribution is a better fit for the data. A p -value less than 0.1 means that the value

⁶ \mathfrak{R} is calculated as $\mathcal{R}/(\sigma\sqrt{n})$, where \mathcal{R} is the log-likelihood ratio [10].

of \mathfrak{R} can be trusted to make a conclusion that one candidate distribution (power-law or alternative, depending on the sign of \mathfrak{R}) is a good fit for the data. In contrast, a p -value greater than 0.1 means that there is nothing to be concluded from the likelihood ratio test.

A. Fitting the log-normal distribution to Internet traffic data

Figure 1 shows the results of the LLR test for all 232 traces with log-normal, exponential and Weibull distribution as the alternative to power-law. For this test we have aggregated traffic at a timescale $T = 100$ msec. The points marked with a circle are the ones with $p > 0.1$. It is clear that the log-normal distribution (black line in Figure 1) is the best fit for the studied traces; i.e. $\mathfrak{R} < 0$ and $p < 0.1$ for most traces when the alternative distribution (to the power-law which is almost always rejected) is the log-normal one⁷. The log-normal distribution is not the best fit for 1 out of 27 CAIDA traces, 2 out of 30 Waikato traces, 1 out of 25 Auckland traces, 5 out of 40 Twente traces and 9 out of 110 MAWI traces. We examined these traces in more detail and discuss them in Section III-B.

Both the exponential and Weibull distributions are good fit for some traces but they are not as good as the log-normal distribution, which can fit the vast majority of tested traces.

⁷For clarity, in Figures 1(e) and 2(e) we only plot traces 60 – 110. For traces 1 – 59, \mathfrak{R} is less than 0 and the respective p -value is less than 0.1; i.e. the alternative distribution is the best fit for the respective trace.

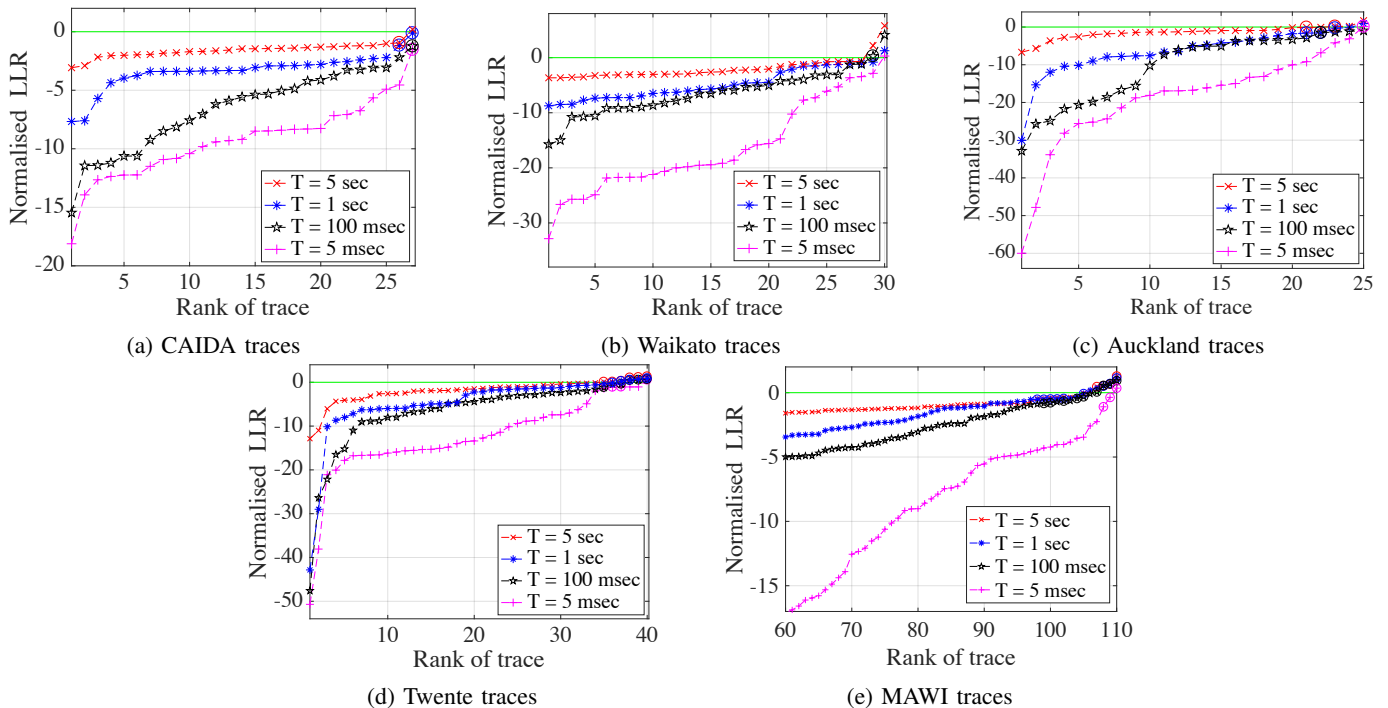


Fig. 2: Normalised Log-Likelihood Ratio (LLR) test results for all studied traces and log-normal distribution. Aggregation timescales are 5 sec, 1 sec, 100 msec and 5 msec. Circled points in the plots are the ones with p -value greater than 0.1, i.e. likelihood test is inconclusive with respect to fitting the log-normal distribution to the traffic data.

Identifying the log-normal distribution as the best fit for the vast majority of traffic traces at $T = 100$ msec is very encouraging. This specific traffic aggregation timescale has been commonly studied in the literature [18], [19].

Next we investigate what the best model is for a range of aggregation timescales. The results are shown in Figure 2. As reflected by the \mathfrak{R} and p -values, the log-normal distribution is the best fit for the vast majority of captured traces at all examined timescales (5 msec to 5 sec)⁸. This is a strong result suggesting the generality of our observations. The good log-normal fit at time scales as small as 5 msec is important for practical applications of the log-normal model.

We also examined Q-Q plots for a large number of traces⁹. The log-normal distribution appeared to be a better fit than other tested distributions and no deviations from the expected pattern were observed in the body or tail of the distribution.

B. Anomalous traces

As mentioned in Section III-A, there is a small number of traces for which the log-normal distribution is not a good fit (none of the other examined distributions is, either). Figure 3(a) shows the probability density function (PDF) plot for one of the 8 anomalous MAWI traces. For comparison,

Figure 3(b) shows the PDF for another MAWI trace for which the log-normal distribution is a good fit. It is obvious from Figure 3(a) that the link was either severely underutilised (see the large spike on the left part of the plot area) or fully utilised (see the smaller spike at the right part of the plot area) for higher data rates. All traces for which the log-normal distribution was not a good fit exhibited similar behaviour and (aggregated) traffic patterns. On the contrary, we did not observe any such behaviour for the majority of traces for which the log-normal distribution was the best fit. A likely explanation for the anomalous traces is that those traces contain either periods of over-capacity (traffic is at 100% of link capacity) or periods where the link is broken (no traffic).

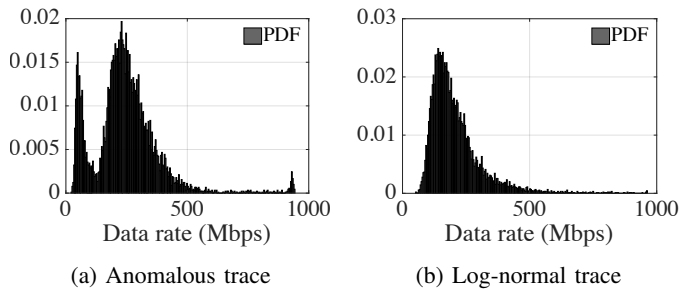


Fig. 3: PDF of an anomalous and non-anomalous trace.

⁸Note that it is possible that the network traffic may not follow a log-normal distribution at very fine or coarse aggregation granularities.

⁹Due to lack of space, Q-Q plots are not included as we would have to present plots for each trace, separately.

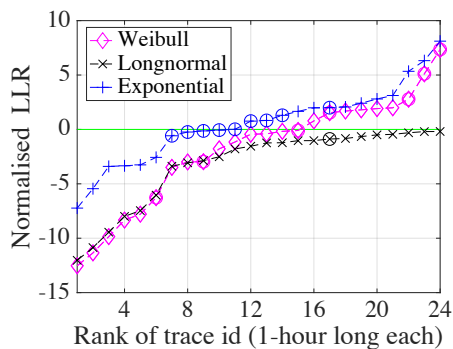


Fig. 4: Normalised LLR test results for the 24 subtraces ($T = 100$ ms) from the 24-hour long Mawi trace. Circled points in the plot are the ones with p -value greater than 0.1 i.e., inconclusive test.

C. Fitting the log-normal distribution to subtraces in the 24-hour long trace

We need to establish whether we can reliably say that the log-normal distribution is a good fit for any sample length of data, not only the 15 minutes long traces (this is discussed in details in Section IV). We apply the power-law test (discussed in Section III) on longer and shorter traces as follows. Firstly, we apply the power-law test on each subtrace (1-hour long) of the 24-hour long Mawi trace. Figure 4 shows the results of the LLR test on 24 subtraces. These results complement our results on the 15 minutes long traces (see Figure 1) by showing that the log-normal distribution is the best fit for these subtraces. There is only one trace (trace id 17 in Figure 4) where neither the log-normal nor the other tested distributions provide a good fit. This trace was captured at time 17:00-18:00. The PDF of this trace has two peaks (it looks similar to the PDF shown in Figure 9), which requires a bimodal distribution to fit. However, when divided this subtrace into two 30 minutes long sections the log-normal distribution was a good fit to each section separately. Secondly, we apply the power-law test on small groups from a 1-hour long Mawi trace. We picked data points from this trace using different time windows: 2, 3, 4 and 5 minutes. This means that each group contains 30, 20, 15 and 12 subtraces, respectively. Figure 5 shows the power-law test results on all these groups when using log-normal. The results show that log-normal is a good fit for all of these small subtrace groups at all tested windows.

D. Fitting the log-normal and Gaussian distributions using the correlation coefficient test

The linear correlation coefficient test has been widely used to assess the fit of a distribution to empirical data. To reinforce the results of Section III-A, we assess the fit of the log-normal and Gaussian distributions to all studied traces. We use the linear correlation coefficient as defined in [20]:

$$\gamma = \frac{\sum_{i=1}^n (S_{(i)} - \hat{\mu})(x_i - \hat{x})}{\sqrt{\sum_{i=1}^n (S_{(i)} - \hat{\mu})^2 \cdot \sum_{i=1}^n (x_i - \hat{x})^2}} \quad (1)$$

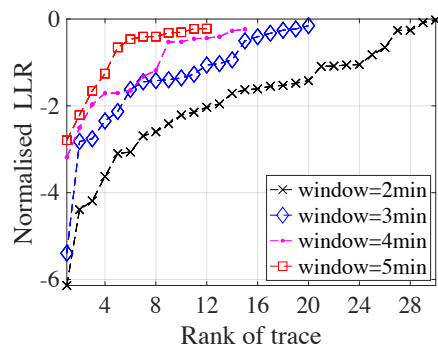


Fig. 5: Normalised LLR test results for different groups from the 1-hour long Mawi trace. Each group contains different number of small traces based on the window size.

where $S_{(i)}$ is the observed sample i , $\hat{\mu} = \frac{1}{n} \sum_{i=1}^n S_{(i)}$ is the samples' mean value, and x_i is sample i from the reference distribution (log-normal in our case), which can be calculated from the inverse cumulative distribution function (CDF) of the reference random variable $x_i = F^{-1}\left(\frac{i}{n+1}\right)$ and $\hat{x} = \frac{1}{n} \sum_{i=1}^n x_i$ is the respective mean value. The value of the correlation coefficient can vary between $-1 \leq \gamma \leq 1$, with a 1, 0 and -1 indicating perfect correlation, no correlation and perfect anti-correlation, respectively. Strong goodness-of-fit (GOF) is assumed to exist when the value of γ is greater than 0.95 [18].

We measure the linear correlation coefficient for all datasets at four different aggregation timescales (ranging from 5 msec to 5 sec) and plot the results in Figures 6(a) to 6(e) for the log-normal distribution and Figures 6(f) to 6(j) for the Gaussian distribution. Traces are ordered by the value of γ for the given timescale. It can be clearly seen that $\gamma > 0.95$ for most traces when employing the test for the log-normal distribution, but this is not the case for the Gaussian distribution. γ is larger for smaller aggregation timescales indicating that the log-normal distribution is an even better fit as the aggregation gets finer. For very small values of T , i.e. lower than 1 msec, data samples exhibit binary behaviour, where either a packet is transmitted or not during each examined time frame [19]. We have examined γ for very short (and large) aggregation timescales, and can confirm the absence of a model describing the data (for brevity, we have omitted the relevant figures).

Next, we calculate v_γ (the variation of γ) for each dataset. v_γ gives an indication of the stability of γ for each dataset, for all timescales tested. This metric is defined as:

$$v_\gamma = \sqrt{\text{var}(\gamma_{T_1}, \gamma_{T_2}, \gamma_{T_3}, \gamma_{T_4})} \quad (2)$$

where $T_1 = 5$ sec, $T_2 = 1$ sec, $T_3 = 100$ msec and $T_4 = 5$ msec. Figures 6(k) to 6(o) show the results for each dataset with the traces ranked by v_γ . For log-normal model, v_γ is very small (below 0.045) for all traces, therefore we can conclude that γ is almost constant for all studied aggregation timescales. While v_γ is higher for the Gaussian model. Furthermore, the error bars in Figures 6(p) to 6(t) represent the standard

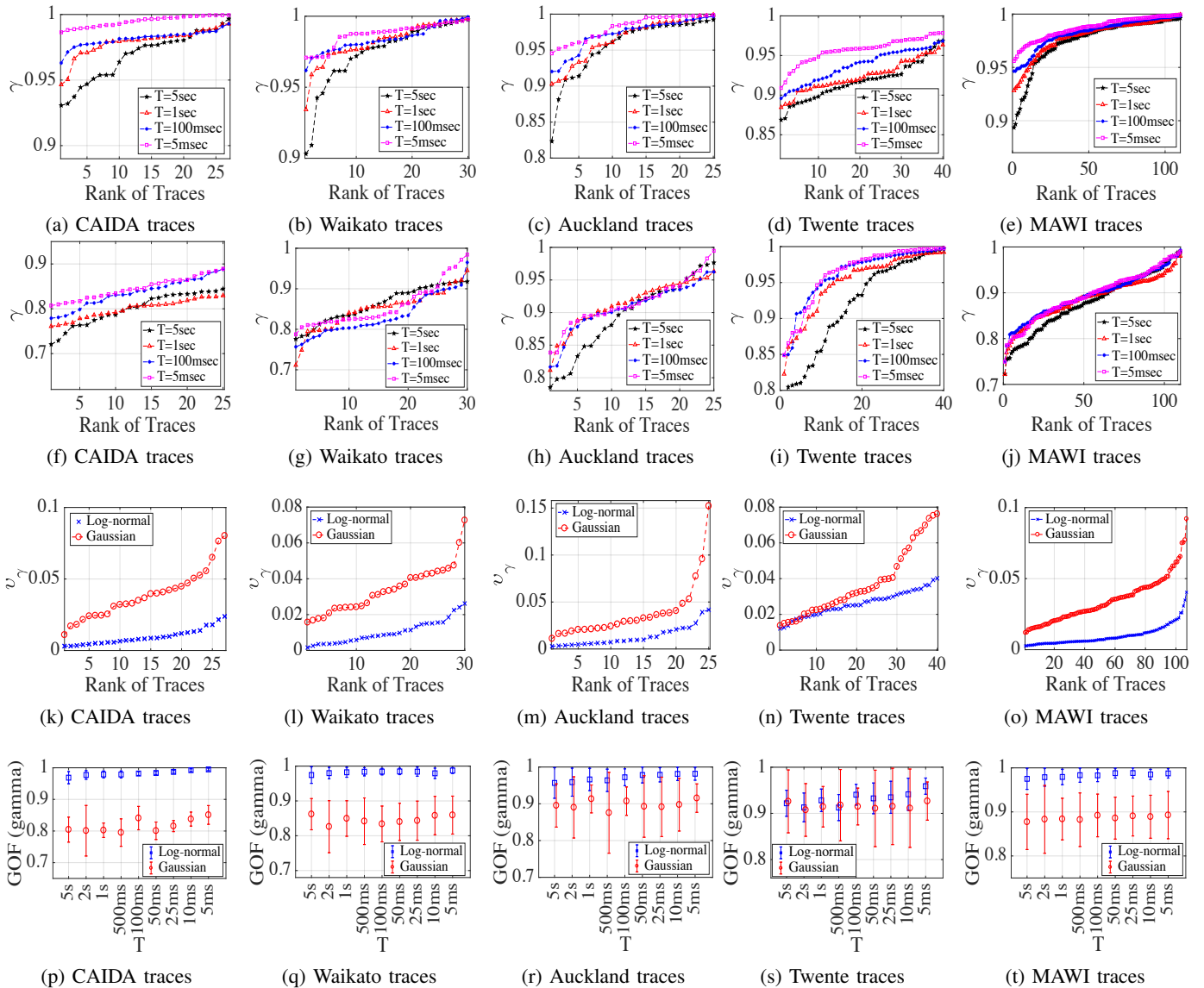


Fig. 6: Correlation coefficient test results for all studied traces and different timescales.

deviation of the correlation coefficient at different timescales (see x-axis). This again shows that for the log-normal model γ is larger than 0.95 (at different T values) for most CAIDA and MAWI traces, while it is larger than 0.9 for all other datasets. This is not the case with the Gaussian model, where most γ values are less than 0.9.

Overall, the correlation coefficient test reinforces the results extracted in Section III-A, providing strong evidence that the log-normal distribution is the best fit for all studied traces. The superior performance of our model can also be seen from comparison of our results for correlation coefficient with those in [21] where the Gaussian model was used.

IV. STATIONARITY TESTING

Stationarity plays an important role in time series analysis [22]–[24]. The study of Internet traffic as a time series depends

mainly on two factors. Firstly, a time period over which to study the traffic and secondly a timescale that is used to aggregate the traffic over a specific time period. If the aggregation timescale is very small then the “volume” will really be a product of exactly how many packets are classified as arriving within that period leading to very noisy measurement. If the time period is longer, however, our measured time period will contain very few samples and the statistics calculated will lack power to reject hypotheses, producing instead inconclusive results simply because they have insufficient data. Ideally therefore we want the time period we study to be as long as possible. However, over long time periods, we know the mean volume is subject to change due to diurnal behaviour of the users. Hence we want to establish whether we can reliably say that a sample of 15 minutes of data is typically stationary

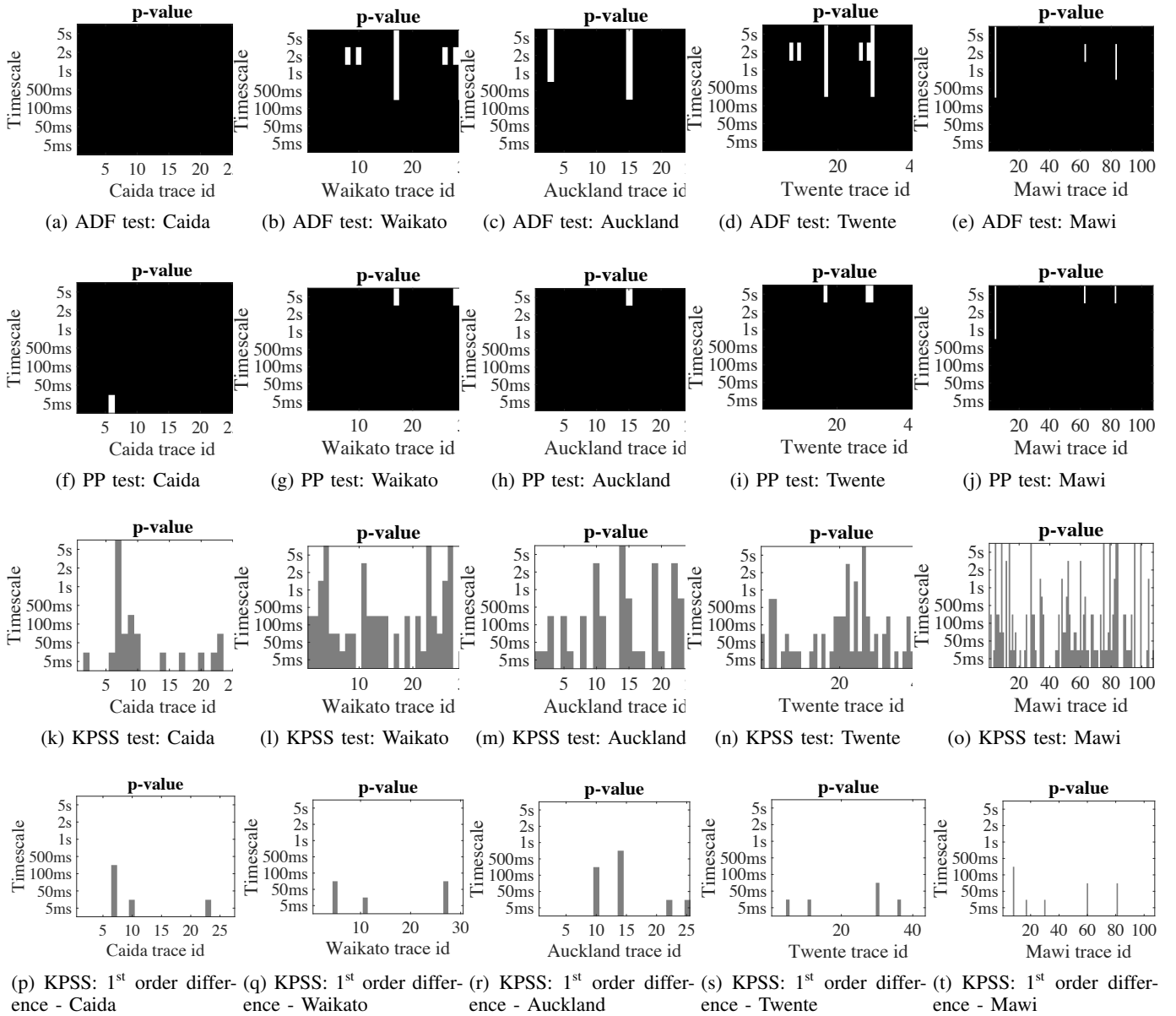


Fig. 7: Stationarity tests' results of the 15-minute long traces. Black: stationary, grey: non-stationary, white: inconclusive. In ADF and PP tests, the black areas represent $p\text{-value} \leq 0.05$ (stationary results), while the white areas represent $p\text{-value} > 0.05$ (inconclusive results). In KPSS test, the grey areas represent $p\text{-value} \leq 0.05$ (non-stationary results), while the white areas represent $p\text{-value} > 0.05$ (inconclusive result) (see Table I).

in this data set. We conclude that this is usually the case except for the anomalous traces.

We examine traffic stationarity using the traces discussed in Section II at different timescales using three tests commonly used for stationarity testing, namely the Augmented Dickey-Fuller (ADF) [25], Phillips-Perron (PP) [26] and Kwiatkowski-Phillips-Schmidt-Shin (KPSS) [27] tests. In the ADF and PP tests, the *null* hypothesis is that a *unit root* is present and the alternate hypothesis is *stationarity*. In the KPSS test, the *null* hypothesis is that the time series is *stationary* and the alternate hypothesis is that a *unit root* is present. Table I summarises

the hypotheses of the three tests and outlines the outcome of each test according to the $p\text{-value}$.

A. Stationarity tests of 15-minute long traces

We begin by conducting the stationarity tests on the 232 15-minute long traces (described in Section II). We aggregate the original data at different timescales; larger aggregation scales (e.g. 5 sec) have fewer data points. Table II shows the average number of data points used in the stationarity tests for each dataset. Figure 7 shows the stationarity results for the ADF, PP and KPSS tests at different aggregation timescales (5 ms, 50 ms, 100 ms, 500 ms, 1 sec, 2 sec and 5 sec).

TABLE I: ADF, PP and KPSS tests

	ADF and PP tests	KPSS test
null hypothesis (H0)	unit root is present	series is stationary
alternative hypothesis (H1)	series is stationary	unit root is present
p -value > 0.05	H0 is not rejected: result is inconclusive	H0 is not rejected: result is inconclusive
p -value ≤ 0.05	H0 is rejected: series is stationary	H0 is rejected: series is non-stationary (due to a unit root)

According to the ADF and PP tests (Figures 7(a-j)), the majority of time series are stationary for all aggregation timescales; the p -value is less than 0.05 (shown as black areas in the figures), therefore the *null* hypothesis is rejected and there is enough evidence to support the alternative hypothesis. There are a few traces for which the p -value is greater than 0.05 at some aggregation timescales (shown as white areas in the figures). For these traces the null hypothesis cannot be rejected. These are the *anomalous traces* discussed in Section III-B. Below, we employ the KPSS test to provide evidence that these series are non-stationary; i.e. to show that for the studied traffic traces, where the log-normal was not a good fit for a specific trace, the underlying time series was not stationary. As shown in Figure 3, said traces appear with a bi-modal distribution.

When performing the KPSS test (Figures 7(k) to 7(o)), we fail to reject the null hypothesis for most traces, as the p -value is larger than 0.05 (shown as white areas in the figures - inconclusive results). For some traces (commonly at small timescales), the null hypothesis is rejected, and therefore there is evidence that the series are non-stationary (grey areas in the figures). KPSS test is sensitive to trends in the time series, so we ran this test by enabling the trend option when testing for stationarity. The problem appears when using small timescales as fluctuations will start to appear, which act as different trends within the time series. For example, applying KPSS test on the trace in Figure 8(a) gives a p -value of 0.01 i.e., the series is non-stationary, however, both ADF and PP tests give p -value equals to 0.001 i.e., the series is stationary. One explanation for the lack of agreement between the tests is due to the presence of trends. These trends may need to be removed prior to modelling. Differencing is a method of transforming a time series dataset that can be used to remove the series dependence on time, including structures like trends and seasonality [28]. Figure 8(b) shows the first-order difference of the trace that is shown in Figure 8(a). We re-run the KPSS test again on the first-order difference series. This gives a p -value of 0.1, i.e., we fail to reject the stationarity null hypothesis. Figures 7(p) to 7(t) show that we always fail to reject the stationarity null hypothesis for most traces (at the tested timescales) in our datasets when applying the KPSS test on the first-order difference sequences (i.e., the results are inconclusive). In general, it is important to realise that the results of the KPSS test and the results of ADF and PP seem contradictory at shorter timescales. Technically, when $p \leq 0.05$, the ADF and PP tests show evidence that the time series has a root within the unit circle, which is equivalent to saying that the time series either is stationary or the first difference is stationary. We test this by using the KPSS test on the first difference of

TABLE II: Average number of points used in the stationarity tests from each dataset at different timescales

Timescale	5 ms	50 ms	100 ms	500 ms	1 sec	2 sec	5 sec
Caida	478545	77850	28925	9955	4470	2570	1010
Waikato	398660	39866	19933	3987	1993	997	399
Auckland	252389	25239	12620	2524	1262	631	253
Twente	180001	18000	9000	1800	900	450	180
Mawi	179755	17975	8988	1798	899	449	180

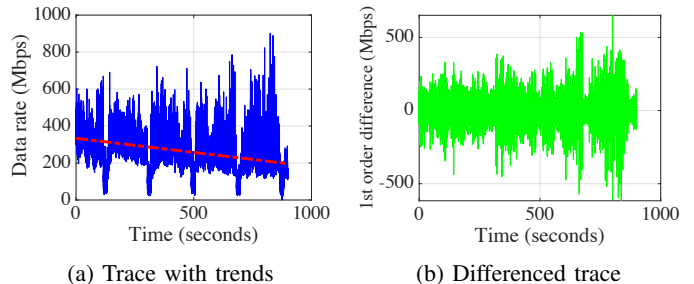


Fig. 8: First-order differencing of a Mawi trace with trends.

the time series. The results that are shown in Figure 7(k-o) are consistent with the conclusion that the data is stationary at longer aggregations: 0.5 – 5s and first-difference stationary at smaller timescales: 5 – 100ms.

B. Stationarity tests of an hour long samples within a 24-hour trace

In this section we consider the hour-long samples within a 24-hour Mawi trace (described in Section II). This 24-hour long trace is used to see if the assumption of stationarity holds for periods longer than 15 minutes. We conclude that these are also stationary.

Figures 9 and 10 show the data rate plots as PDF and as a time series, respectively. It is obvious that the 24-hour long series is not stationary; for example, the average data rate in

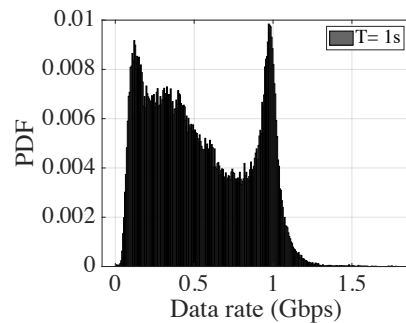


Fig. 9: 24-hour Mawi trace: PDF.

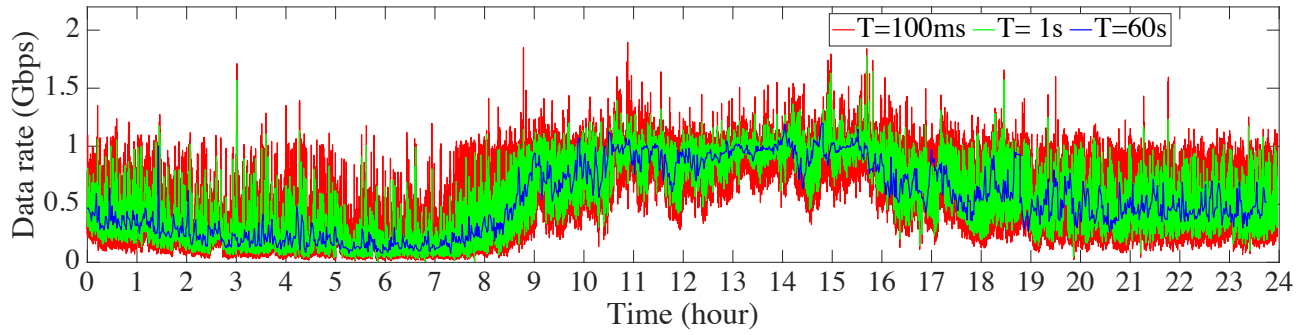


Fig. 10: 24-hour long Mawi trace

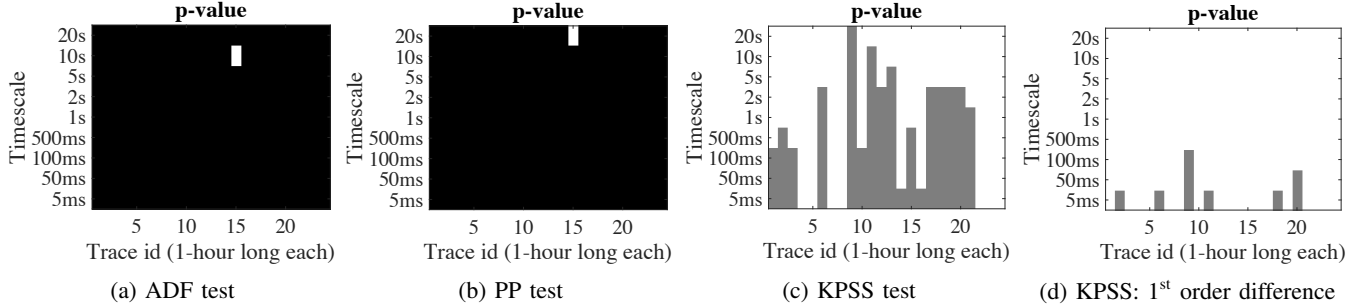


Fig. 11: Stationarity tests' results of 24 1-hour long subtraces from the 24-hour long Mawi trace. Black: stationary, grey: non-stationary, white: inconclusive. In ADF and PP tests, the black areas represent $p\text{-value} \leq 0.05$ (stationary results), while the white areas represent $p\text{-value} > 0.05$ (inconclusive results). In KPSS test, the grey areas represent $p\text{-value} \leq 0.05$ (non-stationary results), while the white areas represent $p\text{-value} > 0.05$ (inconclusive result) (see Table I).

this series between 12:00 am to 05:00 am is 0.252 Gbps, while the average in the time period between 09:00 am to 17:00 pm is 0.875 Gbps.

We run the stationarity tests for this traffic trace and for different aggregation timescales at different sampling times. We start by applying ADF, PP and KPSS tests on 1-hour long groups (subtraces) in this trace (the time at each group or subtrace starts at the beginning of each hour). The stationarity tests results are shown in Figure 11. It is clear from the the first two tests' results that the majority of the 1-hour long groups are stationary (black areas in the figure) as their null hypothesis is rejected. The KPSS test shows many subtraces (white areas) where we failed to reject the null hypothesis i.e., inconclusive results. We ran the KPSS test on the first-order difference series (white areas in Figure 11(d)) and the number of contradictory results was greatly reduced as the KPSS test failed to reject the null-hypothesis of trend stationarity.

It is worth mentioning that these results might slightly change for some groups if we use 1-hour long groups that do not start at the beginning of each hour (e.g., when using a 1-hour long group that starts at 08:30 am, as a jump in the captured data rate will appear at the second half of this group causing it to be non-stationary).

Now, we run the stationarity tests on all the data points in this 24-hour long trace at different sampling times. Table III shows the number of points that have been used from this trace at different timescales. We would expect this 24-hour long time

TABLE III: The number of data points used in the stationarity tests in the 24-hour long Mawi trace at different timescales

Timescale	100 ms	500 ms	1 sec	10 sec	20 sec	60 sec
#points	862724	172554	86283	8639	4325	1449

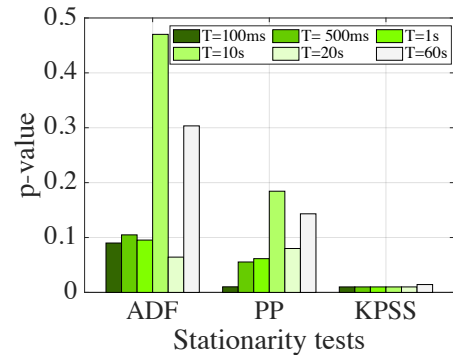


Fig. 12: 24-hour Mawi trace stationarity results.

series to be non-stationary. Figure 12 shows the stationarity tests results of this 24-hour long Mawi trace. The $p\text{-values}$ of ADF and PP tests are larger than 0.05 at all timescales (except at $T = 100$ ms for PP test), which is consistent with non-stationarity. Similarly, the $p\text{-values}$ of KPSS test are smaller than 0.05, which indicates the rejection of the null hypothesis i.e., the series is non-stationary.

V. BANDWIDTH PROVISIONING

It has been previously suggested that network link provisioning could be based on fitted traffic models instead of relying on straightforward empirical rules [21]. In this way, over- or under-provisioning can be mitigated or eliminated even in the presence of strong traffic fluctuations. Such approaches rely on having a statistical model that accurately describes the network traffic. This is therefore an excellent area for applying our findings on fitting the log-normal distribution to Internet traffic data. In the literature, the following inequality (the authors call it the “link transparency formula”) has been used for bandwidth provisioning [19]:

$$P(A(T) \geq CT) \leq \varepsilon. \quad (3)$$

In words, this inequality states that the probability that the captured traffic $A(T)$ over a specific aggregation timescale T is larger than the link capacity has to be smaller than the value of a performance criterion ε . The value of ε is chosen carefully by the network provider in order to meet a specific SLA [21]. Likewise, the value of the aggregation time T should be sufficiently small so that the fluctuations in the traffic can be modelled as well, taking into account the buffering capabilities of network switching devices¹⁰.

We compare bandwidth provisioning using Meent’s approximation formula [21] (assuming Gaussian) and using a log-normal traffic model.

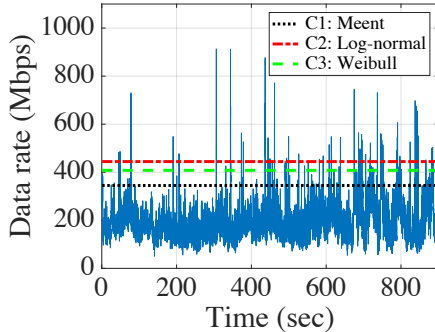


Fig. 13: Data rate of a MAWI trace ($T = 100$ msec and $\varepsilon = 0.01$). The horizontal lines represent the calculated link capacity based on different models.

A. Bandwidth provisioning using Meent’s formula

To find the minimum required link capacity, Meent et al. [21] proposed a bandwidth provisioning approach that is based on the assumption that the traffic follows a Gaussian distribution. Meent’s dimensioning formula is defined as follows [21]:

$$C1 = \mu + \frac{1}{T} \sqrt{-2 \log(\varepsilon) \cdot v(T)} \quad (4)$$

¹⁰Large traffic fluctuations at very short aggregation timescales are smoothed by the presence of buffers at network routers and switches.

where μ is the average value of the traffic, $v(T)$ is the variance at timescale T and ε is the performance criterion. The link capacity is obtained by adding a safety margin value

$$\text{Safety margin} = \sqrt{-2 \log(\varepsilon)} \cdot \sqrt{\frac{v(T)}{T^2}}$$

to the average of the captured traffic (see Equation 4). This safety margin value depends on ε and the ratio $\sqrt{v(T)/T^2}$. As the value of ε decreases the safety margin increases. For example, when the value of ε decreases from 10^{-2} to 10^{-4} , then value of the safety margin increases by 40%. This is different from conventional link dimensioning methods, where the safety margin is fixed to be 30% above the average of the presented traffic [21], [29], [30]. Traffic tails are represented using the Chernoff bound, as follows:

$$P(A(T) \geq CT) \leq e^{-SCT} E[e^{SA(T)}]. \quad (5)$$

Here $E[e^{SA(T)}]$ is the moment generation function (MGF) of the captured traffic $A(T)$.

B. Bandwidth provisioning based on the log-normal model

Here we investigate whether we could achieve more reliable bandwidth provisioning by adopting the log-normal traffic model. We calculate the mean and variance from the captured trace and generate the respective log-normal model. Then, we use the CDF function (F) to solve the link transparency formula shown in Equation 3. Hence, F is defined as $F(C) = P(A(T)/T < C)$, which can be solved to find C , as follows:

$$C2 = F^{-1}(1 - \varepsilon). \quad (6)$$

C. Comparison of bandwidth provisioning approaches

In this section, we compare the bandwidth provisioning approaches described above. The performance indicator is the empirical value of the performance criterion, which is denoted by $\hat{\varepsilon}$ and defined as follows:

$$\hat{\varepsilon} = \frac{\#\{A_i | A_i \geq CT\}}{n}, \quad i \in 1 \dots n. \quad (7)$$

In words, this empirical value is the percentage of all the data samples of the captured traffic which are measured larger than the estimated link capacity. Ideally, $\hat{\varepsilon}$ would be equal to the target value of the performance criterion ε . The difference between $\hat{\varepsilon}$ and ε is due to the fact that the chosen traffic model is not accurately describing the real network traffic. A simple example of the described comparison approach is illustrated in Figure 13, in which we plot the captured data rate for a MAWI trace ($T = 100$ msec)¹¹. The calculated capacity values from each approach when the target ε is 0.01 are $C1 = 344.8$ Mbps and $C2 = 444.3$ Mbps (represented by the horizontal lines in Figure 13). The empirical value can be calculated by using Equation 7, which gives $\hat{\varepsilon}_1 = 0.042$ and $\hat{\varepsilon}_2 = 0.012$. Obviously, with the first approach the network operator would

¹¹Note that in all subsequent figures we have also included results for a Weibull model to get insights about bandwidth provisioning using a heavy-tailed distribution.

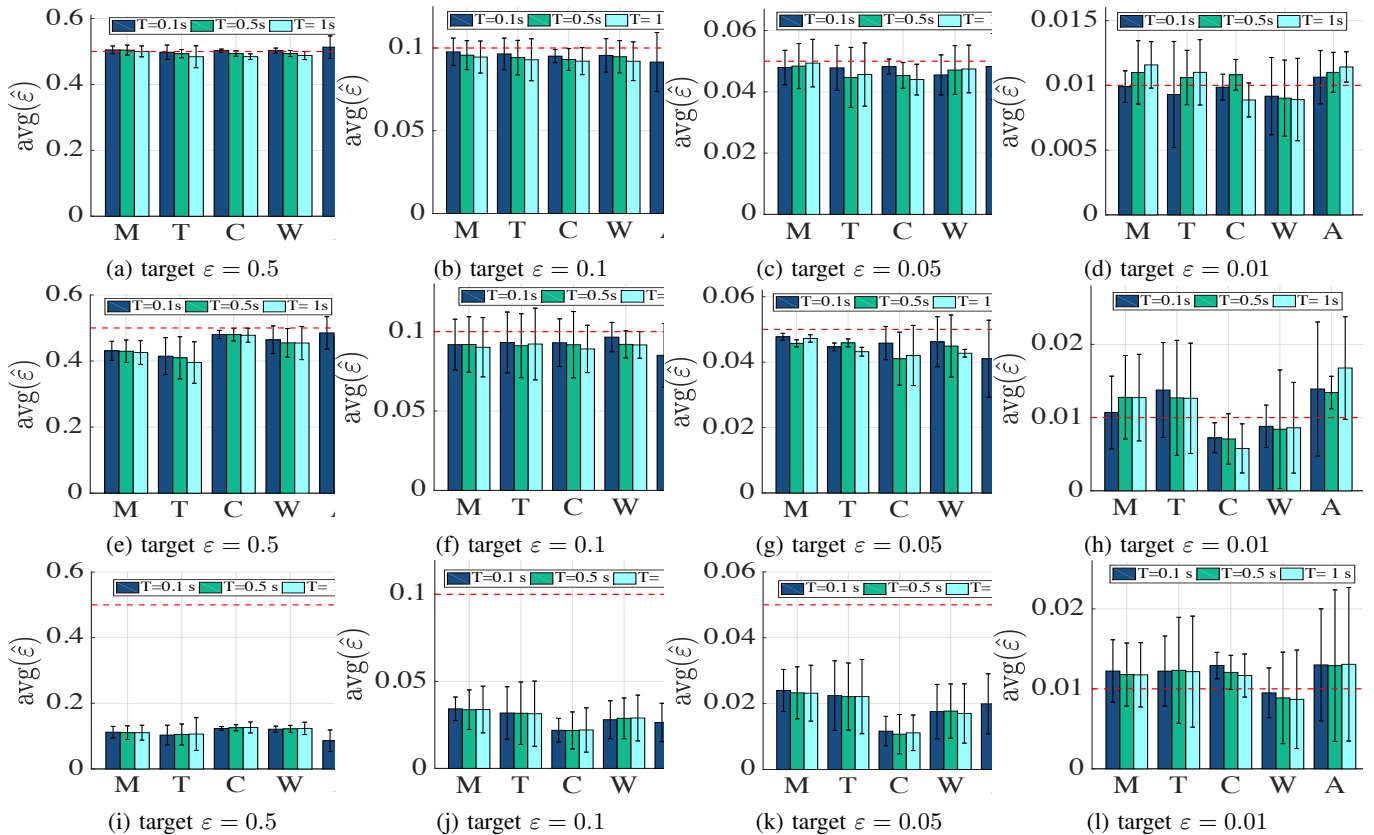


Fig. 14: Link dimensioning based on (a-d) log-normal model, (e-h) Weibull model and (i-l) Meent's formula: $\text{avg}(\hat{\epsilon})$ for different datasets (M: MAWI, T: Twente, C: CAIDA, W: Waikato, A: Auckland), aggregation timescales (100 msec, 500 msec and 1 s), and target values of ϵ (0.5, 0.1, 0.05 and 0.01). Error bars represent $\text{stderr} |\epsilon - \hat{\epsilon}|$.

not be able to meet the target $\epsilon = 0.01$, while with the second approach the empirical value is close to the target.

We next compare results of bandwidth provisioning calculations based on the (a) Meent's formula, (b) Weibull model and (c) proposed log-normal model. Figure 14(a)-(d) shows the average of the empirical value ($\text{avg}(\hat{\epsilon})$) for all traces in each dataset at $T = 0.1$ sec, $T = 0.5$ sec and $T = 1$ sec. The value of T is chosen to be sufficiently small so that the fluctuations in the traffic can be modelled as well. Each model is tested for four different values of the performance criterion: $\epsilon = 0.5$, $\epsilon = 0.1$, $\epsilon = 0.05$ and $\epsilon = 0.01$. In Figure 14(a)-(d) we clearly see that the log-normal model is able to satisfy the required performance criterion ϵ at different aggregation time-scales for all datasets. In contrast, Meent's formula failed to allocate sufficient bandwidth, which results in missing the target performance criterion ϵ for all datasets and target performance values, as depicted in Figure 14(i)-(l) (see horizontal red line). The Weibull distribution performs better comparing to Meent's formula, but bandwidth provisioning using the log-normal model is far superior, as can be seen from Figures 14(a)-(d) and 14(e)-(h).

We apply the same link dimensioning tests as discussed above on 24 subtraces (each one being 1-hour long) from the 24-hour long Mawi trace. Figure 15 shows the $\text{avg}(\hat{\epsilon})$ for all

subtraces at different timescale values. As shown in the figure, the log-normal model performs the best compared to the other two in estimating bandwidth allocation, with respect to the target performance criterion.

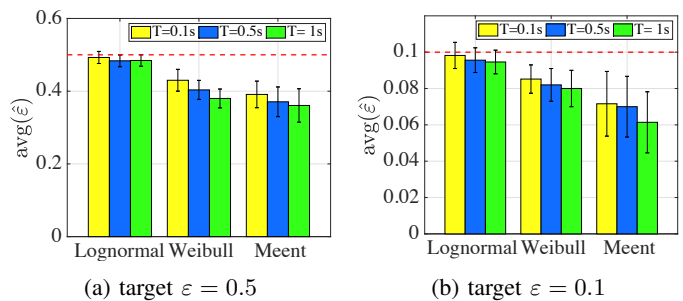


Fig. 15: Link dimensioning based on log-normal, Weibull and Meent's models for 24 subtraces from 24-hour long Mawi trace.

VI. 95TH PERCENTILE PRICING SCHEME BASED ON LOG-NORMAL MODEL

Traffic billing is typically based on the 95th percentile method [31]. Traffic volume is measured at border network devices (typically aggregated at time intervals of 5 minutes)

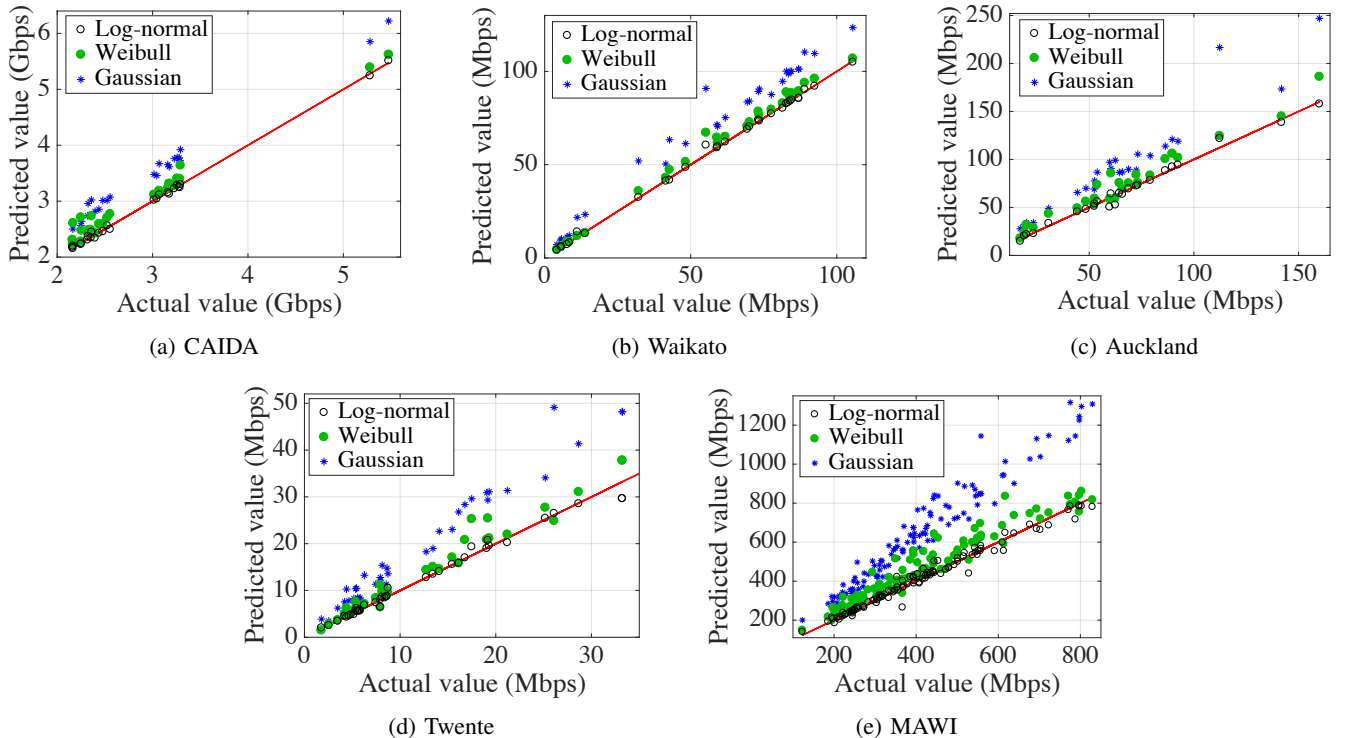


Fig. 16: 95th percentile values (actual vs predicted rates) based on log-normal, Weibull and Gaussian models. An ideal model would result in points in the plot area that fall exactly on the red line.

and bills are calculated according to the 95-percentile of the distribution of measured volumes; i.e. network operators calculate bills by disregarding occasional traffic spikes. Forecasting future bills, which is important for ISPs and clients, can be done using a model of the traffic calculated through previously sampled traffic. In this section, we apply our findings on Internet traffic modelling in predicting the cost of traffic according to the 95th percentile method.

For each network trace we calculate the actual 95th percentile of the traffic volume. The majority of the studied traffic traces were 15-minute long but operators typically use measurements traffic volumes for much longer periods, therefore we scale down the calculation of the 95th percentile by dividing each trace (900 seconds) into 90 groups (10 seconds length each).

In reality, of course, the 95th percentile method would use traffic from different times of day with different means which would need to be modelled as separate log normal distributions with separate means and variances. This is not possible with the fifteen minute long samples that form the focus of this paper. However, it remains a level playing field test for which of the distributions best captures the real underlying data.

We calculate the 95th percentile for the observed traffic. We then fit a Gaussian, Weibull and log-normal distribution to each trace (for $T = 100$ msec) and calculate the 95th percentile of the fitted distribution. We plot the actual 95th percentile against the three predictions in Figure 16 with a red reference line to show where perfect predictions would be located. It is clear that the log-normal model provides much more accurate

TABLE IV: Goodness of fit (GOF) using Normalised Root Mean Squared Error (NRMSE)

Model/Dataset	CAIDA	Waikato	Auckland	Twente	MAWI
Log-normal	0.0399	0.0401	0.1058	0.0979	0.1528
Weibull	0.2410	0.1148	0.2984	0.2123	0.4145
Gaussian	0.5544	0.4193	0.6866	0.5741	0.9828

predictions of the 95th percentile than the Gaussian model. As with the bandwidth dimensioning case discussed in Section V, the Weibull is better than the Gaussian model but worse than the proposed log-normal model.

We employ the normalised root mean squared error (NRMSE) as a goodness of fit to the results in Figure 16. NRMSE measures the differences between values predicted by a hypothetical model and the actual values. In other words, it measures the quality of the fit between the actual data and the predicted model. Table IV shows the NRMSE for all datasets and the three considered models. It is clear that the lowest NRMSE value is for the log-normal model, which is the best model compared to the Gaussian and Weibull ones.

We apply the same 95th percentile test on each 1-hour long subtrace from the 24-hour long Mawi trace. For each 1-hour long subtrace, we calculated the 95th percentile by dividing each subtrace (1 hour) into 60 groups (1 minute long each). Figure 17 shows the results for the 24 subtraces. The log-normal model is significantly more accurate in predicting the 95th percentile compared to the Weibull and Gaussian models.

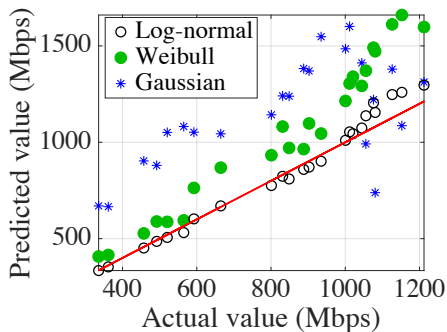


Fig. 17: 95th percentile values based on different models for 24 subtraces from 24-hour long Mawi trace.

VII. RELATED WORK

Reliable traffic modelling is important for network planning, deployment and management; e.g. for traffic billing and network dimensioning. Historically, network traffic has been widely assumed to follow a Gaussian distribution. In [5], [7], the authors studied network traces and verified that the Gaussianity assumption was valid (according to simple goodness-of-fit (GOF) tests they used) at two different timescales. In [32], the authors studied traffic traces during busy hours over a relatively long period of time and also found that the Gaussian distribution is a good fit for the captured traffic. Schmidt et al. [8] found that the degree of Gaussianity is affected by short and intensive activities of single network hosts that create sudden traffic bursts. All the above mentioned works agreed on the Gaussian or ‘fairly Gaussian’ traffic at different levels of aggregations in terms of timescale and number of users. The authors in [20], [33] examined the levels of aggregation required to observe Gaussianity in the modelled traffic, and concluded that this can be disturbed by traffic bursts. The work in [9], [34] reinforces the argument above, by showing existence of large traffic spikes at short timescales which result in high values in the tail. Compared to existing literature, our findings are based on a modern, principled statistical methodology, and traffic traces that are spatially and temporally diverse. We have tested several hypothesised distributions and not just Gaussianity.

An early work drawing attention to the presence of heavy tails in Internet file sizes (not traffic) is that of Crovella and Bestavros [2]. Deciding whether Internet flows could be heavy-tailed became important as this implies significant departures from Gaussianity. The authors in [35] provided robust evidence for the presence of various kinds of scaling, and in particular, heavy-tailed sources and long-range dependence in a large dataset of traffic spanning a duration of 14 years.

When modelling network traffic, many authors did not perform any tests for stationarity, assuming that their traces are realisations of a weakly stationary stochastic process [36], [37]. Other authors consider non-stationary behaviour of traffic observations [24], [38]. The authors in [39], [40] show that traffic patterns have almost deterministic daily variations resulting in clear non-stationary behaviour on a day timescale.

The authors in [38] demonstrated that multiplexed traffic on a high-speed link may have non-stationary behaviour and discussed possible causes of non-stationarity of traffic observations. They argue that this could be due to time-varying number of aggregated sources, routing changes or specific aggregation of a constant number of stationary sources. A common approach in traffic modelling is to choose sufficiently small blocks of observations such that observations in separate blocks are expected to be at least weakly stationary [18], [23], [41]. For example, when testing for applicability of the Gaussian model to traffic modelling authors in [20] neglected a part of their trace claiming that it may introduce undesirable non-stationary behaviour. Authors in [24] assumed that 5-minute blocks of their traffic observations are sufficient to ensure intra-block stationarity.

Understanding the traffic characteristics and how these evolve is crucial for ISPs for network planning and link dimensioning. Operators typically over-provision their networks. A common approach to do so is to calculate the average bandwidth utilisation [6] and add a safety margin. As a rule of thumb, this margin is defined as a percentage of the calculated bandwidth utilisation [29]. Meent et al. [21] proposed a new bandwidth provisioning formula, which calculates the minimum bandwidth that guarantees the required performance, according to an underlying SLA. This approach relies on the statistical parameters of the captured traffic and a performance parameter. The underlying fundamental assumption for this to work is that the traffic the network operator sees follows a Gaussian distribution. Same approach has been used in [19].

The 95th percentile method is used widely for network traffic billing. Dimitropoulos et al. [31] have found that the computed 95th percentile is significantly affected by traffic aggregation parameters. However, in their approach they do not assume any underlying model of the traffic; instead, they base their study on specific captured traces. Stanojevic et al. [4] proposed the use of Shapley value for computing the contribution of each flow to the 95th percentile price of interconnect links. Works [42]–[45] propose calculating the 95th percentile using experimental approaches. Xu et al. [46] assume that network traffic follows a Gaussian distribution “through reasonable aggregation” and propose a cost-efficient data centre selection approach based on the 95th percentile.

VIII. CONCLUSION

The distribution of traffic on Internet links is an important fundamental problem that has received relatively little attention. We use a well-known, state-of-the-art statistical framework to investigate the problem using a large corpus of traces. The traces cover several network settings including home user access links, tier 1 backbone links and campus to Internet links. The traces are from times from 2002 to 2020 and are from a number of different countries. We investigated the distribution of the amount of traffic observed on a link in a given (small) aggregation period which we varied from 5ms to 5s. The hypotheses compared were that the traffic volume was heavy-tailed, that the traffic was log-normal and that the

traffic was normal (Gaussian). The vast majority of traces fitted the log-normal assumption best and this remained true for all timescales tried. Where no distribution tested was a good fit this could be attributed either to the link being saturated (at full capacity) for a large part of the observation or exhibiting signs of link-failure (no or very low traffic for part of the observation).

We tested the data for the hypothesis of stationarity. Over long periods (hours and days) the data is not stationary as it is subject to daily and weekly behaviour related to human activity. Over a fifteen minute or one hour period our tests show that the data is stationary when aggregated at timescales of 500ms to 5s and is first-difference stationary when aggregated at smaller time-scales from 5ms to 100ms.

We investigate the impact of the distribution on two sample traffic engineering problems. Firstly, we looked at predicting the proportion of time a link will exceed a given capacity. This could be useful for provisioning links or for predicting when SLA violation is likely to occur. Secondly, we looked at predicting the 95th percentile transit bill that ISP might be given. For both of these problems the log-normal distribution gave a more accurate result than a heavy-tailed distribution or a Gaussian distribution. We conclude that the log-normal distribution is a good (best) fit for traffic volume on normally functioning internet links in a variety of settings and over a variety of timescales, and further argue that this assumption can make a large difference to statistically predicted outcomes for applied network engineering problems.

REFERENCES

- [1] P. Pruthi and A. Erramilli, "Heavy-tailed on/off source behavior and self-similar traffic," in *Proc. of ICC*, 1995.
- [2] M. E. Crovella and A. Bestavros, "Self-similarity in world wide web traffic: evidence and possible causes," *IEEE/ACM ToN*, 1997.
- [3] P. Loiseau, P. Goncalves, G. Dewaele, P. Borgnat, P. Abry, and P. V. B. Primet, "Investigating self-similarity and heavy-tailed distributions on a large-scale experimental facility," *IEEE/ACM ToN*, 2010.
- [4] R. Stanojevic et al., "On economic heavy hitters: Shapley value analysis of 95th-percentile pricing," in *Proc. of ACM IMC*, 2010.
- [5] R. V. D. Meent, M. Mandjes, and A. Pras, "Gaussian traffic everywhere?" in *Proc. of IEEE ICC*, 2006.
- [6] R. d. O. Schmidt, H. van den Berg, and A. Pras, "Measurement-based network link dimensioning," in *Proc. of IFIP/IEEE*, 2015.
- [7] R. d. O. Schmidt, R. Sadre, and A. Pras, "Gaussian traffic revisited," in *Proc. of IFIP Networking*, 2013.
- [8] R. d. O. Schmidt, R. Sadre, N. Melnikov, J. Schnwlder, and A. Pras, "Linking network usage patterns to traffic gaussianity fit," in *Proc. of IFIP Networking*, 2014.
- [9] X. Yang, "Designing traffic profiles for bursty Internet traffic," in *Proc. of IEEE GLOBECOM*, 2002.
- [10] A. Clauset, C. S. Rohilla, and M. Newman, "Power-law distributions in empirical data," *arXiv:0706.1062v2*, 2009.
- [11] M. Alasmar, G. Parisi, R. Clegg, and N. Zakhleniuk, "On the distribution of traffic volumes in the internet and its implications," in *Proc. of IEEE INFOCOM*, 2019.
- [12] "The caida uscd anonymized internet traces," 2016. [Online]. Available: http://www.caida.org/data/passive/passive_dataset.xml
- [13] "Mawi archive," 2018. [Online]. Available: <http://mawi.wide.ad.jp/>
- [14] R. R. R. Barbosa, R. Sadre, A. Pras, and R. van de Meent, "Simpleweb/university of twente traffic traces data repository," <http://eprints.eemcs.utwente.nl/17829/>, Twente uni, Tech. Rep., 2010.
- [15] "Wits: Waikato internet traffic storage," 2013. [Online]. Available: <https://wand.net.nz/wits/waikato/8/>
- [16] "Wits: Auckland x," 2009. [Online]. Available: <https://wand.net.nz/wits/auck/10/>
- [17] J. Alstott, E. Bullmore, and D. Plenz, "powerlaw: a python package for analysis of heavy-tailed distributions," *arXiv:1305.0215*, 2014.
- [18] M. Mandjes and R. van de Meent, "Resource dimensioning through buffer sampling," *IEEE/ACM Transactions on Networking*, 2009.
- [19] R. d. O. Schmidt, R. Sadre, A. Sperotto, H. van den Berg, and A. Pras, "Impact of packet sampling on link dimensioning," *IEEE Transactions on Network and Service Management*, 2015.
- [20] J. Kilpi and I. Norros, "Testing the gaussian approximation of aggregate traffic," in *Proc. of SIGCOMM*, 2002.
- [21] A. Pras, L. Nieuwenhuis, R. van de Meent, and M. Mandjes, "Dimensioning network links: a new look at equivalent bandwidth," *IEEE Network*, 2009.
- [22] G. Lauks, A. Skrastins, and J. Jelinskis, "Testing the null hypothesis of stationarity of internet traffic," *Elektronika ir Elektrotechnika*, 2011.
- [23] D. Moltchanov, "Modeling local stationary behavior of internet traffic," in *Journal of Communications Software and Systems*, 2008.
- [24] J. Cao, W. S. Cleveland, D. Lin, and D. X. Sun, "On the nonstationarity of internet traffic," in *ACM SIGMETRICS*, ser. SIGMETRICS '01, 2001.
- [25] D. Dickey and W. Fuller, "Distribution of the Estimators for Autoregressive Time Series With a Unit Root," *JSTOR*, 1979.
- [26] P. C. B. Phillips and P. Perron, "Testing for a Unit Root in Time Series Regression," *Journal of the American Statistical Association*, 1988.
- [27] D. Kwiatkowski, P. C. B. Phillips, P. Schmidt, and Y. Shin, "Testing the null hypothesis of stationarity against the alternative of a unit root," *Journal of Econometrics*, 1992.
- [28] R. Hyndman and G. Athanasopoulos, "Forecasting: Principles and practice," in *OTexts: Melbourne, Australia*, <https://otexts.com/fpp2/>, 2018.
- [29] "Best practices in core network capacity planning," online, accessed July 2018. [Online]. Available: https://www.cisco.com/c/en/us/products/collateral/routers/wan-automation-engine/white_paper_c11-728551.pdf
- [30] M. Alasmar and N. Zakhleniuk, "Network link dimensioning based on statistical analysis and modeling of real internet traffic," *arXiv:1710.00420*, 2017.
- [31] X. Dimitropoulos, P. Hurley, A. Kind, and M. P. Stoeklin, "On the 95-Percentile Billing Method," in *Proc. of PAM*, 2009.
- [32] J. L. García-Dorado, J. A. Hernández, J. Aracil, J. E. López de Vergara, and S. Lopez-Buedo, "Characterization of the busy-hour traffic of IP networks based on their intrinsic features," *Computer Networks*, 2011.
- [33] A. B. Downey, "Evidence for Long-tailed Distributions in the Internet," in *Proc. of ACM SIGCOMM Workshop on Internet Measurement*, 2001.
- [34] H. Abrahamsson, B. Ahlgren, P. Lindvall, J. Nieminen, and P. Tholin, "Traffic characteristics on 1gbits access aggregation links," in *Proc. of IEEE ICC*, 2017.
- [35] R. Fontugne et al., "Scaling in internet traffic: A 14 year and 3 day longitudinal study, with multiscale analyses and random projections," *IEEE/ACM Transactions on Networking*, 2017.
- [36] W. E. Leland, M. S. Taqqu, W. Willinger, and D. V. Wilson, "On the self-similar nature of Ethernet traffic," in *IEEE/ACM ToN*, 1994.
- [37] W. Willinger, M. S. Taqqu, R. Sherman, and D. V. Wilson, "Self-similarity through high-variability: statistical analysis of Ethernet LAN traffic at the source level," *IEEE/ACM ToN*, 1997.
- [38] T. Karagiannis, M. Molle, M. Faloutsos, and A. Broido, "A nonstationary poisson view of internet traffic," in *IEEE INFOCOM 2004*, 2004.
- [39] K. Thompson, G. J. Miller, and R. Wilder, "Wide-area internet traffic patterns and characteristics," *IEEE Network*, 1997.
- [40] V. Paxson and S. Floyd, "Wide area traffic: the failure of poisson modeling," *IEEE/ACM Transactions on Networking*, 1995.
- [41] M. Yajnik, Sue Moon, J. Kurose, and D. Towsley, "Measurement and modelling of the temporal dependence in packet loss," in *Proc. of IEEE INFOCOM*, 1999.
- [42] L. Golubchik et al., "To send or not to send: Reducing the cost of data transmission," in *Proc. of IEEE INFOCOM*, 2013.
- [43] N. Laoutaris, M. Sirivianos, X. Yang, and P. Rodriguez, "Inter-datacenter bulk transfers with netstitcher," in *Proc. of ACM SIGCOMM*, 2011.
- [44] I. Castro, R. Stanojevic, and S. Gorinsky, "Using Tuangou to Reduce IP Transit Costs," *IEEE/ACM Transactions on Networking*, 2014.
- [45] H. Xu and B. Li, "Joint request mapping and response routing for geodistributed cloud services," in *Proc. of IEEE INFOCOM*, 2013.
- [46] —, "Cost efficient datacenter selection for cloud services," in *Proc. of IEEE ICC*, 2012.